

Short Communication

A study of Growth Mechanism of Fe Nanowires and Nanotube via Template-Based Electrodeposition

Aiman Mukhtar¹, Babar Shahzad Khan², and Tahir Mehmood^{1,*}

¹ The state key laboratory of Refractories and Metallurgy, Hubei Collaborative Innovation Center for Advanced Steels, International Research Institute for Steel Technology, Wuhan University of Science and Technology, Wuhan, P. R. China

² Department of Physics, Government College Women University, 51310, Sialkot, Pakistan

*E-mail: tahir10621@yahoo.com, aleeza.mukhtar@yahoo.com

Received: 22 November 2016 / Accepted: 17 March 2017 / Published: 12 April 2017

Highly ordered Co nanowire and nanotube arrays were fabricated using anodic aluminum oxide (AAO) templates by DC electrodeposition technique. The Fe microstructures and growth mechanism were investigated using conventional transmission electron microscopy (TEM), Scanning electron microscopy (SEM), X ray diffraction (XRD) method. Two templates with pore size ~50 nm and ~100 nm were prepared, for deposition of nanowires and nanotubes. The material of working electrode and its effect on growth of nanowires and nanotubes was discussed. Our proposed factors i.e. the material of working electrode, pH value, pore diameter and the concentration of metal ions in electrolyte can be useful in future to compose and synthesize other metal nanostructures via template-based electrodeposition.

Keywords: Crystal structure; Nucleation; Growth from solutions; Deposition parameters;

1. INTRODUCTION

Metal nanostructures with nanoscale diameter and high aspect ratio gain attention of research communities from last two decades. They are the bases of fascinating structure-property relationships derived from their 1D confined transport of electrons or photons, quantum confinement, large surface area and excellent mechanical properties, these properties are unique and superior as compared to their bulk counterparts [1-8]. Metal nanowires and nanotubes prepared while using templates assisted method, contains the electrochemical reduction of one or more ions of desirable metals inside the

nano-pore channels of an insulating membrane. The low-cost formation of nanotubes and nanowires in hexagonally ordered pores of AAO templates now has a part of many research works. The shape size structural and magnetic properties are controlled by the changing template and electrodeposition parameters [9-11].

Many researchers [12-15] have studied the growth mechanism of metal nanostructures. Currently lot of theoretical and experimental research work done on metal nanowires, based on nucleation, growth and crystal structure and their impact on surface morphology[11, 12, 16, 17]. Researchers reported that growth of Au, carbon nanotubes and Bi nanowires are helical[18, 19]. Many researchers use Ag or Cu as the working electrode[20, 21] for nanotubes formation and Au is used for nanowires formation[22], but they don't explain the reason why material of working electrode is important for nanowires and nanotubes formation. Chienwen Huang and Yaowu Hao [23] show that Cu form columnar structure on AAO template. They explained that during sputtering some copper atoms migrate in to pores so cup shaped working electrode is formed. Metal starts to grow on this cup shape working electrode and tabular structure is formed[23]. There are very few research reported on growth mechanism of nanotubes[24] compared with nanowires[25-27]. Up till now the growth mechanism of Fe nanowires and nanotubes are unclear, however a full understanding of growth mechanism needs further investigation.

In this study we successfully fabricate the metal nanowires and nanotubes using AAO template and study the growth mechanism of nanowires and nanotubes inside the tubes of AAO template. We believe that there are four factors i.e. the material of working electrode, pH value, pore diameter and the concentration of metal ions in electrolyte, which affect the growth mechanism and help to form nanotubes inside the pores of AAO template.

2. MATERIAL AND METHODS

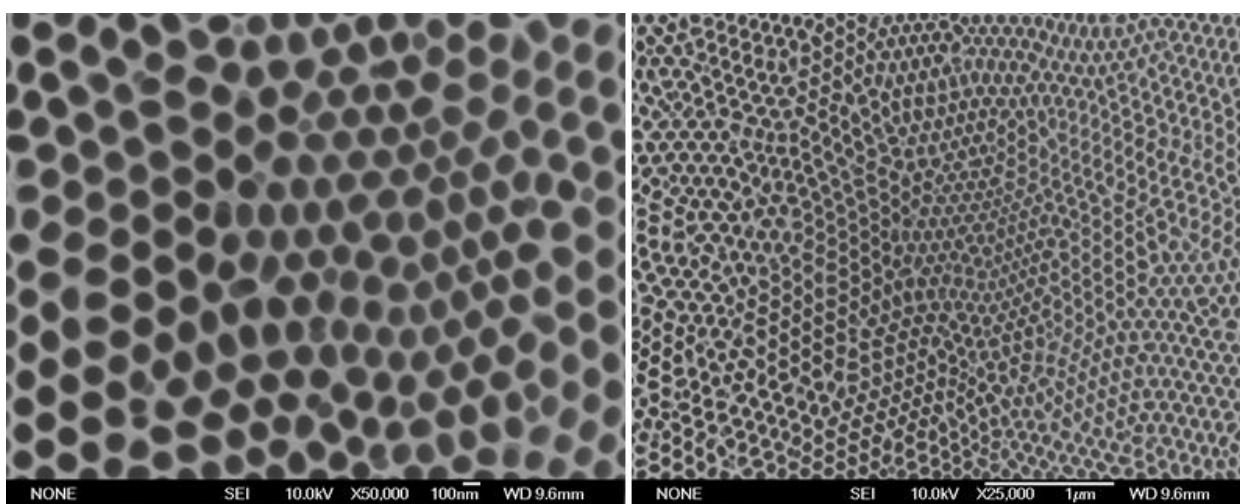


Figure 1. Hexagonally arranged pores of AAO template with pore size of (a) ~50 nm (b) ~100 nm

The detailed experimental procedure for preparation of AAO templates is given in our previous paper. Here different anodization conditions is discussed to obtain desired pore size.

1) Aluminium foils were anodized in a 0.4 M H₂C₂O₄ solution for 6 hours which forms pores with diameter of ~100nm. A DC voltage of 45 V was used between the electrodes. The temperature was 2°C to 5°C sustained by using a refrigeration system. To remove the alumina layer formed in the first anodization, these foils were dissolved in a solution of chromic acid (1.8 wt %) and phosphoric acid (6 wt %) at 60°C. To achieve an ordered nanoporous layer, a second anodization process was done on the substrate. The same arrangement with the same parameters and electrolyte were used just anodization time was kept 12 hours for this step. The hexagonally arranged and ordered honeycomb pores was formed as shown in fig.1a

2) For nanowires formation, the same two anodization procedure was repeated. Here 0.4 M H₂SO₄ was used which create pores in a diameter range of 30-50. A DC voltage of 25 V was used between the electrodes. The hexagonally arranged and ordered honeycomb pores was formed as shown in fig.1b. Table.1 shows the required parameters of AAO template used for obtaining desired pore diameter of nanotubes and nanowires.

Table 1. shows the required parameters of AAO template for nanowires and nanotubes formation.

Composition Of Electrolyte	Concentration Of Electrolyte	Applied Voltage (V)	Temperature (°C)	Pore Diameter (nm)	
(COOH) ₂	0.4 M	45	0±2	80-100	nanotubes
H ₂ SO ₄	0.4 M	25	0±2	30-50	nanowires

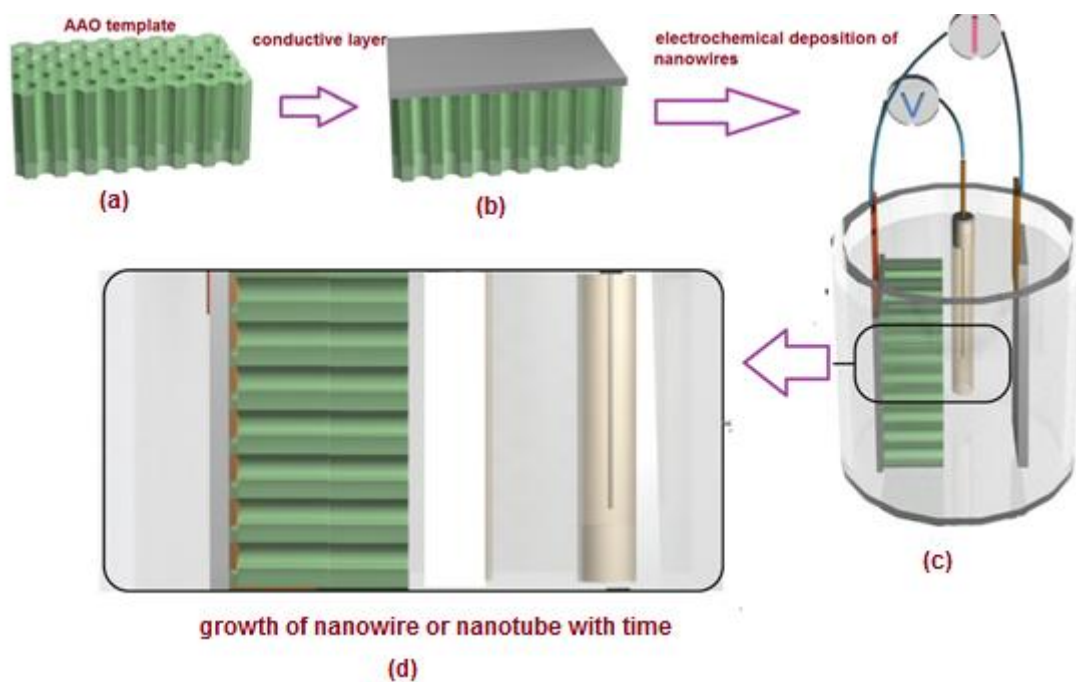


Figure 2. Schematic illustration of (a) AAO template (b) Sputtered conductive layer(c) electrodeposition of alloy nanowires and nanotubes (d) growth of alloy nanowires and nanotubes with time

The electrolyte used was $0.3MFeSO_4 \cdot 7H_2O + 0.65MH_3BO_3$ for nanowires deposition. The *pH* of electrolyte was adjusted to 2.5 by adding 1M H_2SO_4 solution. For nanotubes deposition electrolyte used was $0.284MFeSO_4 \cdot 7H_2O + 0.2MH_3BO_3$, H_2SO_4 was not added so electrolyte has high solution *pH* 5. Both experiments were conducted using -1.6V dc voltage at room temperature as shown in Fig.2. Au and Ag film was sputtered onto the back side of the templates to serve as the working electrode. The reference electrode was the saturated calomel electrode (SCE). The Fe nanowires and nanotubes were analyzed using X-ray diffraction (XRD, X'Pert PRO MRD, PANalytical, Netherlands) with CuK_{α} radiation, scanning electron microscopy (SEM, JEOL JSM-6700F) and transmission electron microscope (TEM, FEI Tecnai G² 20 UTwin).

3. RESULTS AND DISCUSSION

The experimental conditions for preparation of nanotubes are different from preparation of nanowires (in AAO tubes) by following aspects. First, the concentration of metallic ions in the electrolyte was low. Second, H_2SO_4 were not added into the electrolyte to adjust *pH* value and thus the electrolyte has a high *pH* value. Third, template with large pores of ~100 nm in diameter favors the formation of nanotubes. Fourth, for nanotubes formation Ag is used as working electrode and gold was sputtered for nanowire formation. Fig.3 shows the X-ray diffraction (XRD) patterns of 0.356 M Fe nanowires deposited at -1.2V with low solution *pH* 2.5. The XRD data were collected from the top side of nanowires. The Fe nanowires deposited at -1.2V have cubic structure and the preferential growth is on the (110) and (200) plane.

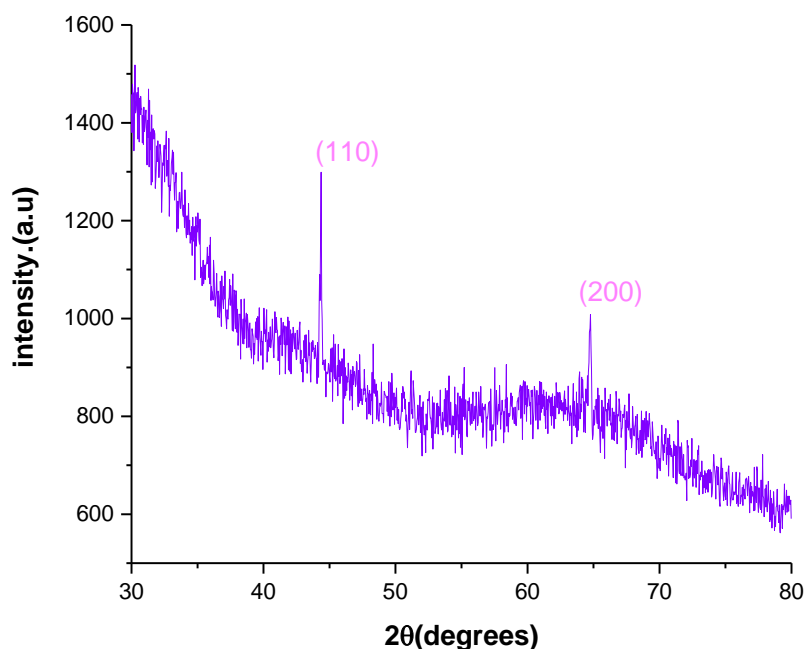


Figure 3. XRD patterns of Fe nanowires deposited at -1.2V in 0.356M solution with *pH* 2.5.

Fig. 4 shows SEM images of Fe nanowires deposited at -1.2V with *pH* 2.5 in 0.356M solution. The diameter (~50nm) of the Fe nanowires is the same as that of the pores of AAO template, indicating that the cylindrical pores of the template were fully filled with Fe atoms.

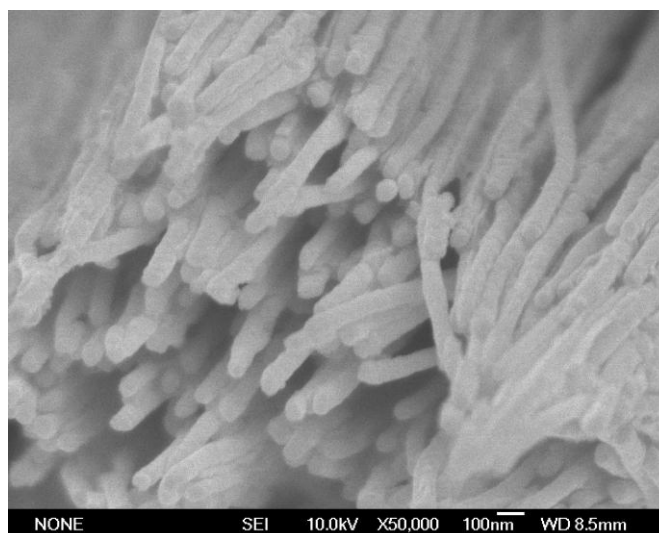


Figure 4. SEM image of Fe nanowires deposited at -1.2V in 0.356M solution with *pH* 2.5.

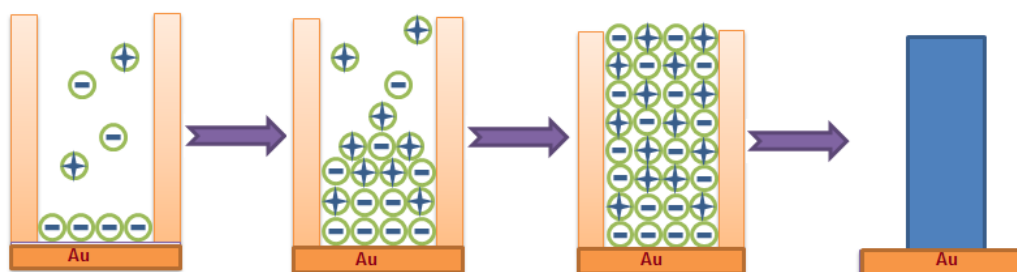


Figure 5. Schematic illustration of growth mechanism of nanowires.

The growth mechanism of nanowires inside pores of AAO tube with using Au electrode is shown in Fig 5. When Au is used as the working electrode with pore diameter ~50 nm, and by using high concentration of metal ions the nanowires grow from the bottom of AAO tube. Metal ions M^{n+} are reduced on Au surface. Then metal atoms nucleate and grow on Au surface; nanowires grow from the bottom. This can be understood by following reason. First, Polycrystalline Au surface have many favorable nucleation sites such as grain boundaries. Second, numerous studies show that when using Au as the working electrode, the head of nanowires (growing surface) are a tip[28, 29]. This indicates that nanowires grow from bottom. This growth behavior also shows that the growth in the central section is faster than outer layer of nanowires. The TEM results show that the protruding tip of nanowires are not completely packed, it means that there are two section of nanowires, one is body which have dense structure and other is tip of nanowire with unpacked structure. Figure 6 shows the TEM image of Fe nanowires, it is clear that the growing surface of metal nanowires is not flat but has protruding tip. Third, the shape of current vs time curves measured during deposition of Co nanowires in our study[11] in agreement with that during deposition of metals on flat substrate[30], the value of

current increases rapidly to the maximum value and then decreases slowly. The time (t_{\max}) requires for achieving N_s (saturation nucleus density) is shorter than one second for depositing [11]. This can indicate that nucleation and growth occurs on Au surface. The Fig.7 (a, b) shows current density vs time curve at the initial time of deposition (0-15sec). In order to check the nucleation and growth occurs on Au surface Fe nanowires are also deposited in high concentration, electrolyte used was $0.71MFeSO_4 \cdot 7H_2O + 0.65MH_3BO_3$ with $-1.2V$ and $pH 2.5$ was used. Curve shows that the, value of maximum current (i_{\max}) increases with increasing Fe ion concentration in the electrolyte and time where current has maximum value(t_m) decreases. At low concentration of $0.356M$ solution t_m and i_{\max} are 1.99 sec -52.07 mA/cm^2 and as we increase the concentration to $0.71M$ the value of t_m decreases to 0.36 sec and value of i_{\max} increases to -109.01 mA/cm^2 , this shows that nucleation and growth occurs on Au surface and Fe nanowires are formed.

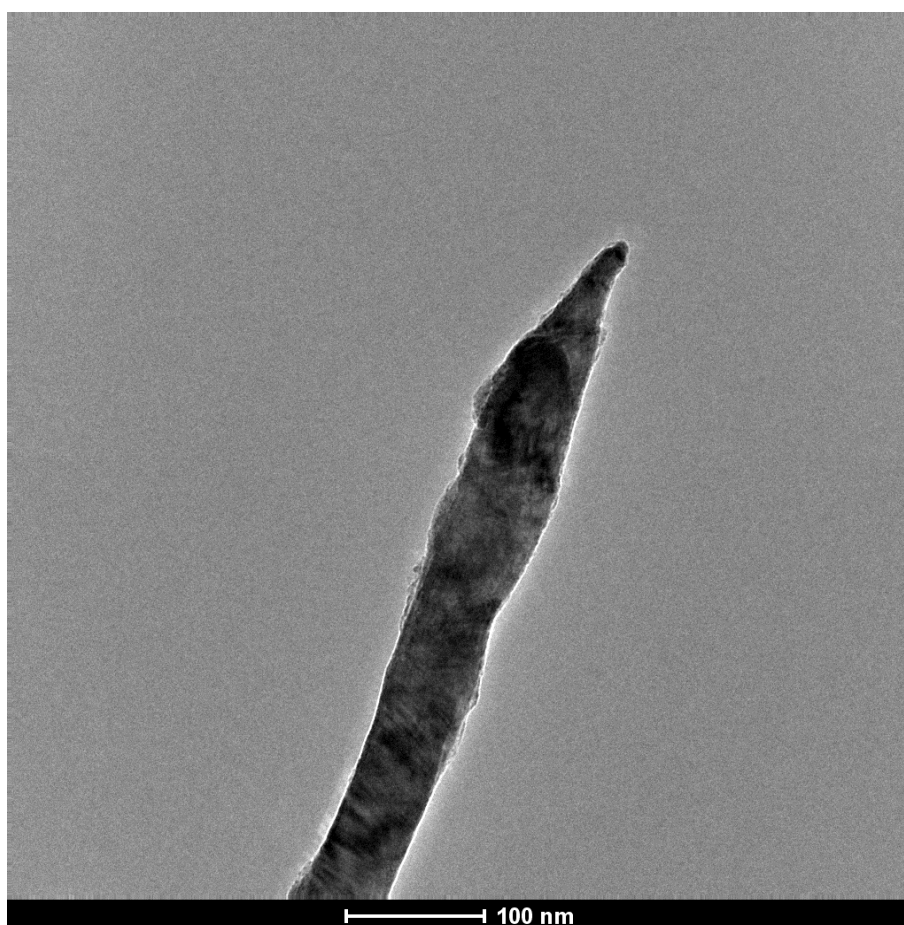


Figure 6. TEM image of nanowires showing the protruding tip of the nanowire

The fig.8 shows schematic illustration of a typical current versus time curve. It is clear from the fig.8 that the current decreases abruptly which is clear in Region I, then nanowires starts to grow from bottom into the pores of the AAO membrane in Region II. The current density remains almost unchanged and metal nanowires grow into the nanopores.

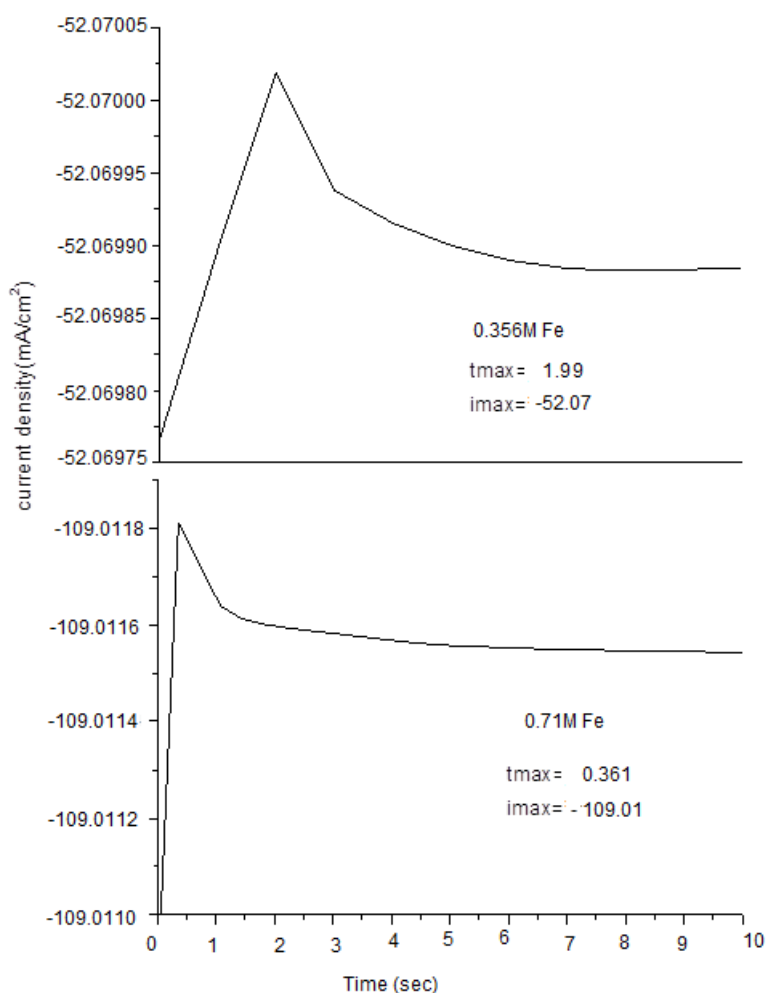


Figure 7. Initial time current density curve at 0.356M and 0.71M Fe at -1.2 V with pH2.5

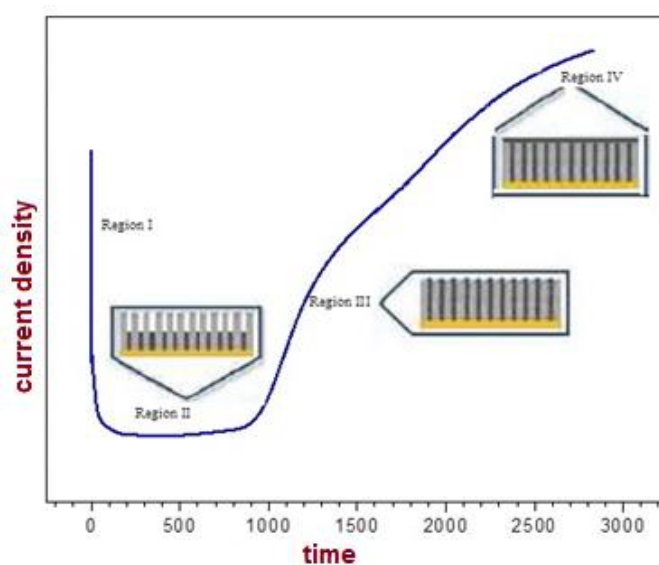


Figure 8. Schematic illustration of current density vs time curve during electrodeposition of metal nanowires

At Region III the electrodeposited material arises to form hemispherical heads above the ends of nanowires and at this time the current density starts to increase rapidly. Region IV is the region of overdeposition where heads reach together cover the surface area of template [31-33].

X-ray diffraction (XRD) patterns of Fe nanowires deposited at -1.2V is shown in Fig. 9. The XRD data were collected from the top side of nanowires. The Fe nanowires deposited at -1.2V have cubic structure and the preferential growth is on the (110), (200) and (220) plane.

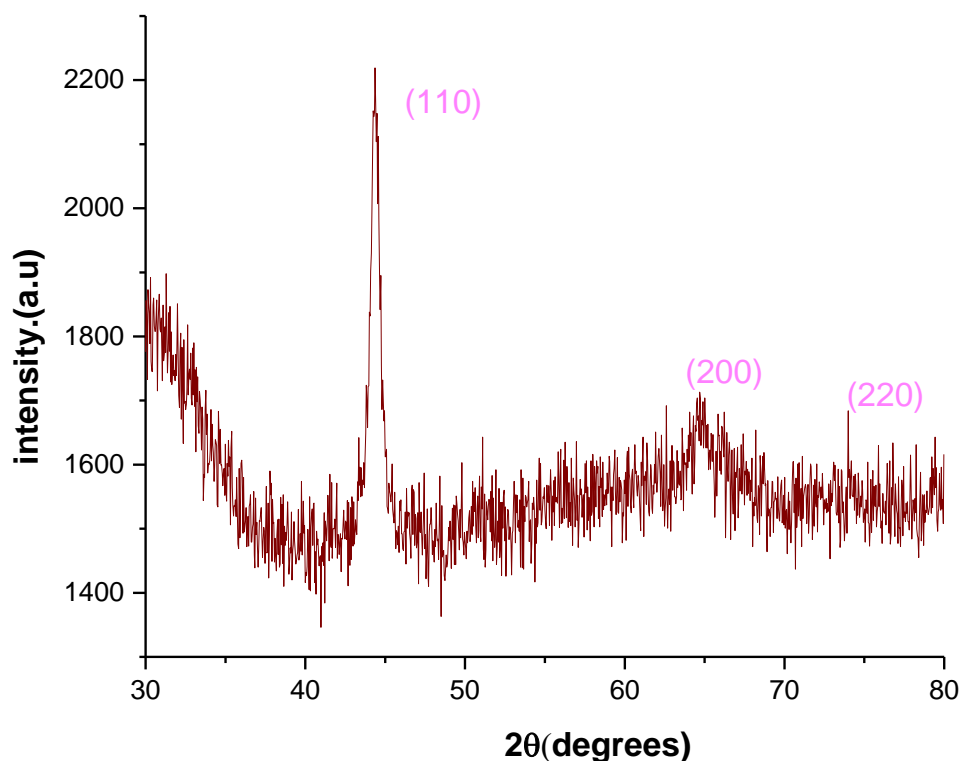


Figure 9. XRD patterns of Fe nanotubes deposited at -1.2V in 0.2 M solution.

Fig. 10(a,b,c) shows SEM and TEM images of Fe nanowires deposited at -1.2V with *pH* 5 in 0.2M solution. The diameter (~100nm) of the Fe nanowires is the same as that of the pores of AAO template, indicating that the cylindrical pores of the template were fully filled with Fe atoms.

Fig.11 shows the growth mechanism of nanotubes, it is clear that the metallic ions grow along the wall of AAO tube. As the inner walls of AAO tubes has surface absorption energy [13, 34], so the surface area of Ag electrode and the bottom edge of AAO tube is used as the preferential site for the deposition of Fe ions. At the initial time of deposition ionized metal moves towards the Ag electrode surface get electron and become atom. Metal atoms combine together to form nanoclusters which absorbed inner walls of nanotubes and tubular structure is formed.

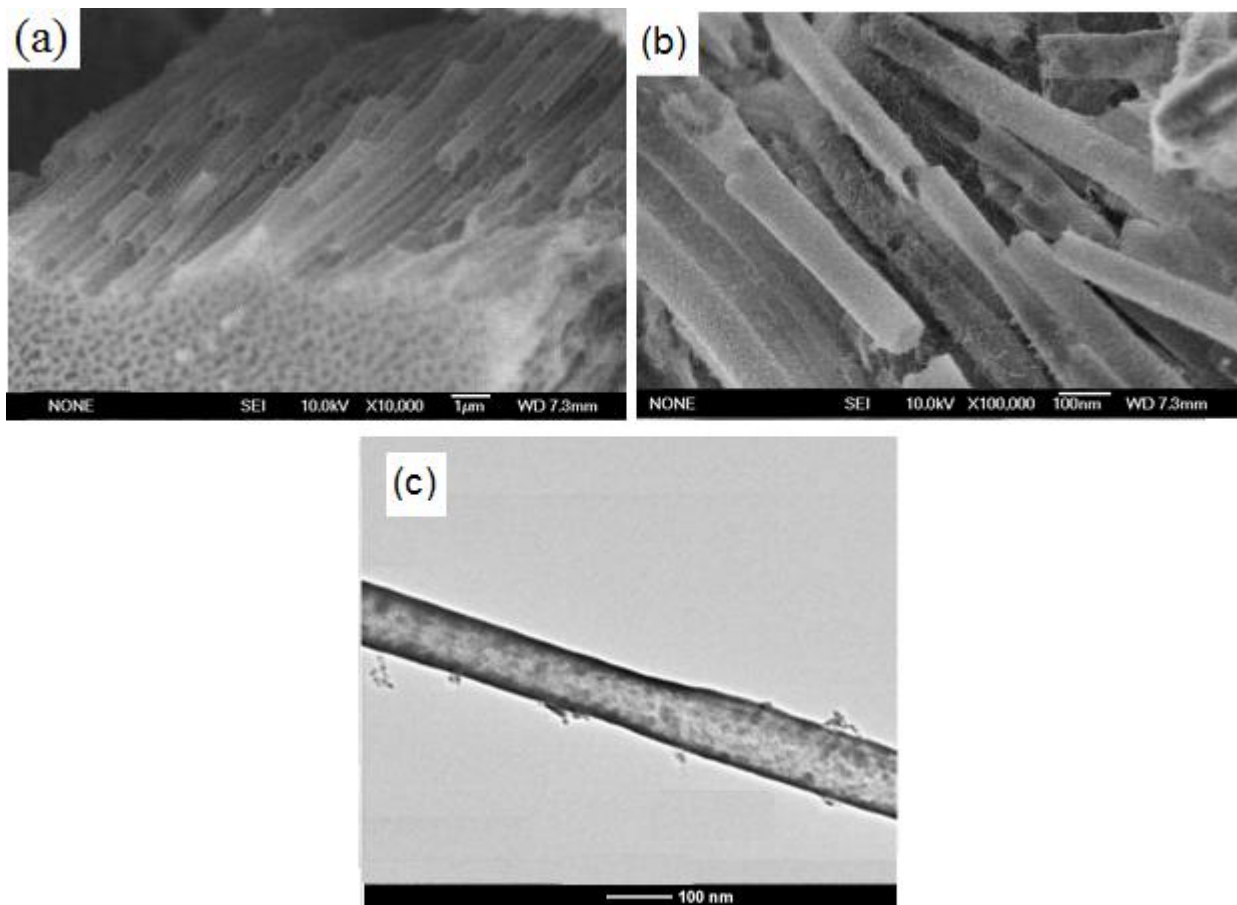


Figure 10. (a) SEM image with 10,000 magnification and (b) SEM image with 100,000 magnification (c) TEM images of Fe nanotubes deposited at -1.2V in 0.2M solution with pH5.

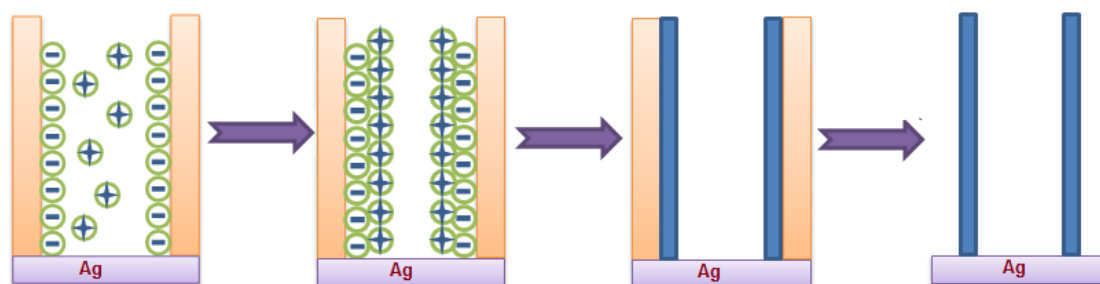


Figure 11. Schematic illustration of growth mechanism of nanotubes.

All metals (except Au and Pt) are oxidized when exposed to air and oxide film with a thickness of several nanometers is formed on the surface of the metals, immediately [35, 36]. Because Au and Pt are not oxidized, Au or Pt is usually used as the working electrode in electrodeposition of metal nanowires. When using Ag or Cu as the working electrode, the oxide film of Ag or Cu can have an effect on the nucleation and growth mode and can lead to the growth along the wall of the AAO tube. For the templates with larger pore of ~100 nm when preparing the working electrode, metal film can form along the internal wall of the AAO template. This favors growth along the wall. Hui-min Zhan et

al[21] believes that potential is the key factor for depositing metal nanowires and nanotubes. They explain that -1.25V is the critical potential at which nanotubes are formed and lower than this value nanowires are formed. We think that they ignore the other deposition parameters which have effect on growth of metal nanowires and nanotubes. Cao et al. [37] have suggested a current directed tubular growth (CDTG) mechanism for nanowires and nanotubes. They showed that metal nanotubes can be formed when growth rate parallel to current direction is greater than growth rate perpendicular to current direction, while nanowires can be formed when growth rate parallel to current direction is approximately equal to growth rate perpendicular to current direction. We believe that this model is difficult to explain the competitive growth rates of nanowires and nanotubes.

Based on the above analysis, the factors which control the growth pattern of nanowires and nanotubes would be: (1) the material of working electrode, (2) The pH value, (3) pore diameter and (4) the concentration of metal ions in electrolyte.

4. CONCLUSION

Highly ordered Fe nanowire and nanotube arrays were fabricated using anodic aluminum oxide (AAO) templates. A growth mechanism of Fe nanowires and nanotubes is discussed. Believe that four factors i.e. the material of working electrode, pH value, pore diameter and the concentration of metal ions in electrolyte contributes the formation nanowires and nanotubes inside the holes of AAO template.

References

1. E. Garnett, P. Yang, *Nano letters*, 10 (2010) 1082
2. R. Yan, D. Gargas, P. Yang, *Nature Photonics*, 3 (2009) 569
3. B. Tian, T.J. Kempa, C.M. Lieber, *Chemical Society Reviews*, 38 (2009) 16.
4. S. Dayeh, A. Gin, S. Picraux, *Applied Physics Letters*, 98 (2011) 163112.
5. Y. Cui, X. Duan, J. Hu, C.M. Lieber, *The Journal of Physical Chemistry B*, 104 (2000) 5213.
6. C.M. Lieber, *Nano letters*, 2 (2002) 81.
7. A. Huczko, *Applied Physics A*, 70 (2000) 365.
8. C.M. Hangarter, N.V. Myung, *Chemistry of Materials*, 17 (2005) 1320.
9. T. Mehmood, B. Shahzad Khan, A. Mukhtar, X. Chen, P. Yi, M. Tan, , *Materials Letters*, 130 (2014) 256
10. T. Mehmood, B.S. Khan, A. Mukhtar, M. Tan, *International Journal of Materials Research*, 106 (2015) 957
11. A. Mukhtar, T. Mehmood, B.S. Khan, M. Tan, *Journal of Crystal Growth*, 441 (2016) 26.
12. H. Pan, B. Liu, J. Yi, C. Poh, S. Lim, J. Ding, Y. Feng, C.H.A. Huan, J. Lin, *The Journal of Physical Chemistry B*, 109 (2005) 3094.
13. M. Lahav, T. Sehayek, A. Vaskevich, I. Rubinstein, *Angewandte Chemie*, 115 (2003) 5734.
14. Q. Wang, G. Wang, X. Han, X. Wang, J.G. Hou, *The Journal of Physical Chemistry B*, 109 (2005) 23326-.
15. C.R. Martin, *Chemistry of Materials*, 8 (1996) 1739.

16. M. Florian, B. Joachim, K. Shafqat, M. Maria Eugenia Toimil, T. Christina, F. Hartmut, *Nanotechnology*, 18 (2007) 135709.
17. D. Jinglai, L. Jie, M. Dan, Y. Huijun, M. Khan, C. Yonghui, S. Youmei, H. Mingdong, Q. Xiaohua, Z. Ling, C. Yanfeng, *Nanotechnology*, 21 (2010) 365605.
18. Y. Oshima, A. Onga, K. Takayanagi, Helical Gold Nanotube Synthesized at 150 K, *Physical Review Letters*, 91 (2003) 205503.
19. E. Tosatti, S. Prestipino, *Science*, 289 (2000) 561
20. T.N. Narayanan, M.M. Shaijumon, P.M. Ajayan, M.R., *The Journal of physical Chemistry C*, 112 (2008) 14281.
21. H.-m. Zhang, X.-l. Zhang, J.-j. Zhang, Z.-y. Li, H.-y. Sun, 160, *Journal of The Electrochemical Society* (2013) D41.
22. B. Shahzad Khan, T. Mehmood, A. Mukhtar, M. Tan, *Materials Letters*, 137 (2014) 13.
23. H. Chienwen, H. Yaowu, *Nanotechnology*, 20 (2009) 445607.
24. X.F. Han, S. Shamaila, R. Sharif, J.Y. Chen, H.R. Liu, D.P. Liu, *Advanced Materials*, 21 (2009) 4619.
25. L. Li, Y. Yang, X. Huang, G. Li, R. Ang, L. Zhang, *Applied physics letters* 88 (2006) 103119.
26. D. Li, R.S. Thompson, G. Bergmann, J.G. Lu, *Advanced Materials* 20 (2008) 4575.
27. X. Li, G. Meng, Q. Xu, M. Kong, X. Zhu, Z. Chu, A.-P. Li, *Nano Letters*, 11 (2011) 1704.
28. M. Tian, J. Wang, J. Kurtz, T.E. Mallouk, M. Chan, *Nano Letters*, 3 (2003) 919.
29. A. Ghahremaninezhad, A. Dolati, *Journal of Alloy and compound*, 480 (2009) 275-278.
30. A. Milchev, L. Heerman, *Electrochimica acta*, 48 (2003) 2903-2913.
31. S. Cheng, C. Huang, *Synthesis and Reactivity in Inorganic, Metal-Organic, and Nano-Metal Chemistry*, 38 (2008) 475.
32. G. Ali, M. Maqbool, *Nanoscale research letters*, 8 (2013) 1.
33. Y. Cao, G. Wei, H. Ge, Y. Yu, *Int. J. Electrochem. Sci*, 9 (2014) 5272.
34. M. Lahav, T. Sehayek, A. Vaskevich, I. Rubinstein, *Angewandte chemie international edition*, 42 (2003) 5576.
35. D.D. Macdonald, *The Point Defect Model for the Passive State*, 139 (1992) 3434-3449.
36. J.W. Schultze, M.M. Lohrengel, *Stability, Electrochimica Acta*, 45 (2000) 2499.
37. H. Cao, L. Wang, Y. Qiu, Q. Wu, G. Wang, L. Zhang, X. Liu, *ChemPhysChem*, 7 (2006) 1500.